All-optical network interface from backbone networks to local area networks based on semiconductor optical amplifiers

Yiyuan Xie (解宜原)[1*] and Zhu Yang (杨 逐)[2]

[1]*School of Electronic and Information Engineering, Southwest University, Chongqing 400715, China*

[2]*College of Education Science, Chongqing Normal University, Chongqing 400047, China*

[*]*Corresponding author: yyxie@swu.edu.cn*

Received June 18, 2013; accepted September 16, 2013; posted online November 4, 2013

We report on the experimental and numerical investigations of an all-optical network interface from backbone networks to local area networks based on semiconductor optical amplifiers (SOAs). All-optical signals at 40 Gbps with return-to-zero (RZ) format in backbone networks are demultiplexed to signals at 10 Gbps with nonreturn-to-zero (NRZ) format in local area networks. SOAs and optical band-pass filters are used in the optical interface. We study the waveform, optical spectrum, and bit error rate (BER) of the interface scheme based on the experimental and numerical simulation results. The interface technique can be used in variable length and bit-rate variable optical networks.

OCIS codes: 060.1155, 060.4510, 230.4480.

doi: 10.3788/COL201311.110605.

Explosive demand on internet traffic requires an innovative networking technology[1,2]. The development of all-optical networks will be a key technology to meet the massive bandwidth requirements of modern communication networks. The evolving trends in optical networks propelled by the continuously increasing bandwidth demands indicate a future that leans toward dense wavelength tributaries, increased line rates (> 40 Gbps), longer transparency length, and improved flexibility. All-optical networks are divided into two parts, namely, backbone networks and local area networks. In general, the transmission speed in backbone networks is extremely high and the code is in return-to-zero (RZ) format. Unlike backbone networks, local area networks typically operate with low-speed nonreturn-to-zero (NRZ) data. RZ formats have been applied to backbone networks because of possible higher tolerance to numerous fiber transmission impairments. Interface techniques between backbone networks and local area networks are attracting significant attention because they employ different transmission speeds and formats[3−10]. In recent years, several groups have proposed various network interface techniques. The operation of optical demultiplexers (DEMUXs) that use optical fibers[11], periodically poled lithium niobates[12], and silicon waveguides[13] has been reported at a bit rate of 320 Gbps or higher. Semiconductor optical amplifiers (SOAs) are also promising candidates for such optical DEMUXs because they provide a smaller footprint, lower switching operation, and higher integration ability compared with other nonlinear devices. Previously, various types of SOA-based optical DEMUXs that use blue-shift filtering[14], symmetric-Mach-Zehnder structures[15,16], and four-wave mixing (FWM)[17] have been developed. Converting RZ to NRZ format is a prominent example of the need for this type of subsystem at the interface between backbone networks and local area networks. Significant efforts have been exerted to apply RZ to NRZ conversion schemes that rely either on Kerr-based nonlinearities, active elements, or linear configurations[18−25].

In this study, we propose and demonstrate an optical interface based on SOAs from backbone networks to local area networks. Limited by the experimental condition, we experimentally and numerically demonstrate a new scheme based on SOAs that can be demulptilexed from 40 to 10 Gbps. Meanwhile, RZ format can be converted into NRZ format. The proposed scheme is robust and has potential applications in optical networks in the future.

A schematic diagram of our experimental setup is shown in Fig. 1. The system consists of a 10-Gbps optical signal generation unit, a decompression unit, and a format conversion unit. In the present experiment, two 10-GHz mode-locked semiconductor lasers were employed for the data and control signal sources. One of the 10-GHz clock sources was modulated by a $LiNbO_3$ modulator (LNM) to generate 10-Gbps data signals. The LNM was driven by a pulse pattern generator with $2^{31}-1$ pseudorandom bit sequence (PRBS) data. The 10-Gbps data signal with a 12-ps pulse width was multiplexed to generate 40-Gbps data signals by using an optical multiplexer (MUX). An optical delay line (ODL) was used to adjust the delay timing between an arbitrary 40-Gbps data channel and the 10-GHz control signal. The signal

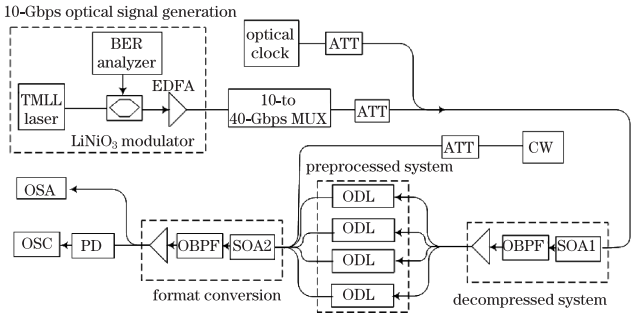

Fig. 1. Schematic diagram of the experimental setup. TMLL: tunable mode-locked laser; PD: photoelectric detector; CW: continue wavelength; OSA: optical spectrum analyzer; OSC: digital oscilloscope.

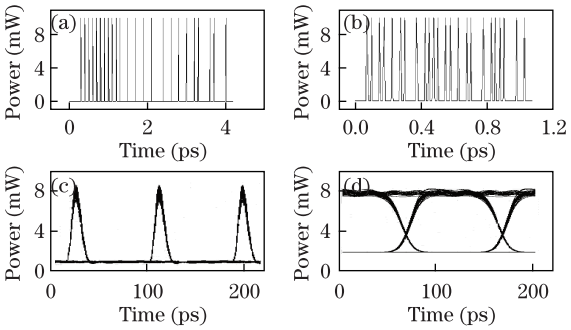

Fig. 2. Waveforms of the optical signal at (a) 10 and (b) 40 Gbps; the eye diagrams of (c) the demultiplexed signal and (d) the NRZ signal after format conversion in the simulation.

Table 1. Parameters Used in the Experiment

Parameter	Value
Wavelength of the RZ Signal at 40 Gbps	1550.16 nm
Wavelength of the Clock Signal	1550.38 nm
Wavelength of the NRZ Signal at 10 Gbps	1559.91 nm
Bit Rate of Input of the Optical RZ Signal	40 Gbps
Injected Current I	250 mA
Small Signal Gain	30 dB
Polarization-dependent Saturated Gain	0.5 dB
Saturation Output	6 dBm
Gain Peak Wavelength	1560 nm
3-dB Spectrum Bandwidth	50 nm
Saturated Gain Recovery Time	25 ps
Carrier Recovery Time	53 ps

was amplified by using an erbium-doped fiber amplifier (EDFA) to adjust the data and control signals injected into the SOA. The data and control signals were combined by an optical coupler and coupled into the all-optical AND logic gate. The gate was based on the SOA and an optical band-pass filter (OBPF). The use of an ultrafast nonlinear process, such as an FWM operation at a bit rate of 40 Gbps, was demonstrated for RZ modulation formats. The all-optical AND logic gate allowed us to extract a corresponding segment from the high-speed signal. The demultiplexed data signal was in RZ modulation format. The demultiplexed data signal was preprocessed by the system which consisted of one power splitter, one power combiner, and four ODLs. The preprocessing system had a time delay of approximately 25 ps in each arm which corresponded to approximately 5.25-mm fiber length difference. The signal power could be controlled by the subsequent optical variable attenuation (ATT)[26]. The signal pulse and the probe light with a central wavelength of 1559.68 nm passed the power combiner and were launched into the SOA. Sufficient RZ signal and probe light were achieved, and the cross-gain modulation (XGM) and cross-phase modulation (XPM) effects induced spectral broadening. The input power of the RZ signal and the probe light could be adjusted by the EDFA and the ATT. Hence, the principle was the XPM and the resultant bit pattern of the NRZ signal. Finally, the subsequent OBPF extracted the sideband spectrum with a central wavelength of approximately 1559.91 nm.

The parameters for the optical interface simulation and experiment are listed in Table 1. We use these parameters to simulate the optical interface scheme. As shown in Fig. 2(a), the low-speed optical signal is a 10-Gbps pulse train at 1550 nm with a 12-ps pulse width. When the signal passes through the MUX, the size of the signal changes from 4 to 1 ns, as shown in Fig. 2(b). When the high-speed signals at 40 Gbps reach the destination node, they can be demultiplexed by the demultiplexed subsystem at 10 Gbps. The eye diagram of the demultiplexed signal at 10 Gbps is presented in Fig. 2(c). To realize format conversion, the system shown in Fig. 1 is used to convert RZ into NRZ at 10 Gbps. The eye diagram of the NRZ signal is shown in Fig. 2(d). As shown in Fig. 2, the optical interface between the core network and local network is realized by using the simulation scheme.

To further study the optical interface, the experimental setup shown in Fig. 1 is used to test and prove the simulation results. The experimental results of the optical interface are presented in Fig. 3. Meanwhile, Fig. 3(a) shows the eye diagram of the original signal at 10 Gbps. In our experiment, the original signal is 10-Gbps pulse train at 1550.16 nm with a 12-ps pulse width. When the original signal passes through the compressor, the speed of the optical signal changes to 40 Gbps, and its eye diagram is shown in Fig. 3(b). This signal is used as the high-speed optical signal in the backbone network. When the signal reaches the interface between the core

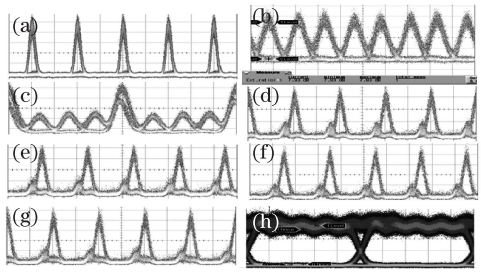

Fig. 3. Eye diagrams of the RZ signal at (a) 10 and (b) 40 Gbps, (c) the clock signal and the RZ signal at 40 Gbps when their positions are aligned, (d)–(g) the demutiplexed signal in the experiment, and (h) the NRZ signal at 10 Gbps.

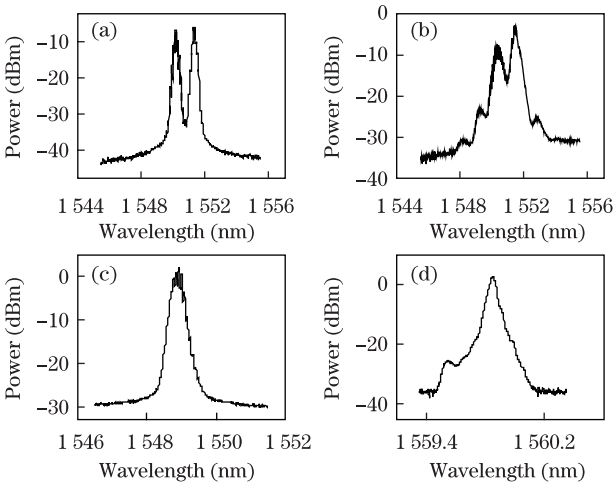

Fig. 4. Optical spectra of the SOA (a) input and (b) output; (c) the RZ signal and (d) the NRZ signal at 10 Gbps in the experiment.

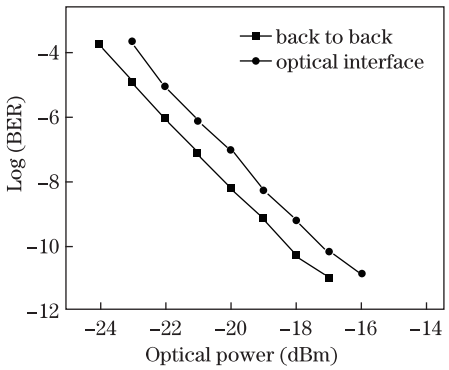

Fig. 5. BER curve of the optical interface.

network and the local network, the demultiplexed and format conversions are used to realize the optical interface, as shown in Fig. 1. In our experiment, the clock signal is a 10-Gbps pulse train at 1551.38 nm with a 12-ps pulse width. The clock signal and the high-speed optical RZ signal at 40 Gbps pass the power combiner, and are launched into SOA1. As shown in Fig. 3(c), the clock signal and the high-speed optical signal achieve sufficient spectral change induced by the FWM effect. Then, the subsequent OBPF extracts the sideband spectrum with a central wavelength of approximately 1549.21 nm. The eye diagrams of the demultiplexed signals are shown in Figs. 3(d)–(g). As shown in these figures, the demultiplexed signals have a "ghost" pulse in the eye diagram because the positions of the clock signal and the RZ signal at 40 Gbps are not aligned precisely. However, the "ghost" pulses do not influence the performance of the optical interface. The 10-Gbps optical signal in the local network is decompressed successfully from a 40-Gbps optical signal in the core network with a clear eye. Then, the 10-Gbps optical RZ signal and the probe light with a central wavelength of 1559.68 nm pass the power combiner and are launched into SOA2. Sufficient RZ signal and probe light were achieved, and the XGM and XPM effects induce spectral broadening. The input power of the signal and the probe light can be adjusted by the EDFA and the ATT. Then, the subsequent OBPF extracts the spectrum with a central wavelength of approximately 1559.91 nm. The eye diagram of the NRZ is shown in Fig. 3(h).

The signal spectra of the SOA used for the optical interface are shown in Fig. 4. The spectra of the 40-Gbps optical signal and the 10-GHz clock signal are shown in Fig. 4(a). When the 40-Gbps optical signal and the 10-GHz clock signal are launched into the SOA, the new optical spectrum is created because of the FWM effect, as shown in Fig. 4(b). The optical spectrum of the 10-Gbps RZ signal is shown in Fig. 4(c). When the central wavelength of the filter is 1559.36 nm, the spectrum of the converted NRZ signal is shown in Fig. 4(d).

The bit error rate (BER) characteristics of the back-to-back interface and the optical interface are shown in Fig. 5. They were performed with 2^{31}–1 long PRBS. From Fig.5, we obtain a BER lower than 10^{-9} when the optical power is larger than –18 dBm. A penalty of approximately 1.3 dB for the optical interface is shown in the Fig. 5.

In conclusion, we successfully demonstrate an optical interface by using nonlinear effects in SOA. We experimentally exhibit that an optical RZ signal at 40 Gbps is decompressed into an optical NRZ signal at 10 Gbps. An average power penalty of less than 1.2 dB is achieved. The results indicate that SOAs have high potential for applications in high-speed optical interfaces.

This work was supported by the National Natural Science Foundation of China (No. 61205088), the Natural Science Foundation of Chongqing City (No. 2011BB2009), the Doctorial Start-up Fund of the Southwest University (No. SWU110030), the Open Research Fund of the State Key Laboratory of Transient Optics and Photonics, the Chinese Academy of Sciences (No. 201003), and the Fundamental Research Funds for the Central Universities (No. XDJK2012B015).

References

1. K. C. Lee and V. O. K. Li, J. Lightwave Technol. **11,** 962 (1993).
2. G. Kramer and G. Pesavento, Commun. Mag. **40,** 66 (2002).
3. A. Saleh and J. Simmons, J. Lightwave Technol. **24,** 3303 (2006).
4. F. Blouin, A. Lee, A. Lee, and M. Beshai, J. Opt. Networking **1,** 56 (2002).
5. T. EI-Bawab and J. Shin, IEEE Commun. Mag. **40,** 60 (2002).
6. A. Banerjee, Y. Park, F. Clarke, H Song, S. Yang, G. Kramer, K. Kim, and B. Mukherjee, J. Opt. Networking **4,** 737 (2005).
7. F. Wang, Y. Yu, X. Huang, and X. Zhang, Photon. Technol. Lett. **21,** 1109 (2009).
8. E. Wong, J. Lightwave Technol. **30,** 597 (2009).
9. Y. Zhan, M. Zhang, M. Liu, L. Liu, and X. Chen, Chin. Opt. Lett. **11,** 030604 (2013).
10. L. Liu, M. Zhang, M. Liu, and X. Zhang, Chin. Opt. Lett. **10,** 070608 (2012).
11. S. Watanabe, R. Okabe, F. Futami, R. Hainberger, C. Schumidt-Langhorst, C. Schubert, and H. G. Weber, in *Proceedings of 30th European Conference on Optical Communication* Th4.1.6 (2004).
12. F. Gomez-Agis, C. M. Okonkwo, A. Albores-Mejia, E. Tangdiongga, and H. J. S. Dorren, Electron. Lett. **46,** 1008 (2010).
13. H. Ji, P. Minhao, G. Michael, K. O. Leif, Y. Kresten, M. H. Jorn, and J. Palle, J. Lightwave Technol. **29,** 426 (2011).
14. E. Tangdiongga, Y. Liu, H. de Waardt, G. D. Khoe, A. M. J. Koonen, and H. J. S. Dorren, Opt. Lett. **32,** 835 (2007).
15. S. Nakamura, Y. Ueno, and K. Tajima, in *Proceedings of Optical Fiber Communication Conference* **FD,** FD3 (2002).
16. T. Hirooka, M. Okazaki, T. Hirano, P. Guan, M. Nakazawa, and S. Nakamura, IEEE Photon. Technol. Lett. **21,** 1574 (2009).
17. S. L. Jansen, M. Heid, S. Spalter, E. Meissner, C. J. Weiske, A. Schopfilin, and H. Waardt, Electron. Lett. **38,** 978 (2002).
18. Z. Hui, J. Zhang, J. Gong, M. Liang, M. Zhang, Y. Yang, F. He, and J. Liu, Opt. Eng. **52,** 055002 (2013).
19. Z. Hui and J. Zhang, J. Opt. **14,** 065402 (2012).
20. S. Bigo, E. Desurvire, and B. Dersuelle, Electron. Lett.

30, 1868 (1994).

21. S. H. Lee, K. K. Chow, and C. Shu, Opt. Express **13,** 1710 (2005).
22. X. Lei, B. C. Wang, V. Baby, I. Glesk, and P. R. Prucnal, IEEE Photon. Technol. Lett. **15,** 308 (2003).
23. C. W. Chow, C. S. Wong, and H. K. Tsang, Opt. Commun. **223,** 309 (2003).
24. X. Zhang, Y. Yu, H. Dexiu, L. Lijun, and F. Wei, IEEE Photon. Technol. Lett. **19,** 1027 (2007).
25. Y. Zhang, E. Xu, D. Huang, and X. Zhang, IEEE Photon. Technol. Lett. **21,** 1202 (2009).
26. Y. Xie, J. Zhang, and W. Wang, J. Mod. Opt. **55,** 3021 (2008).